Trends in Photochemistry & Photobiology
Vol. 14, 2012

Original Communication

Photoreactivity of N-acetyl-7-nitroindolines – Unraveling the mechanism by computation

Jose E. Mendez, Nathan J. Westfall, Katja Michael and Carl W. Dirk*
Department of Chemistry, University of Texas at El Paso, El Paso, TX 79968-0513, USA

ABSTRACT

Photo-cleavable N-acyl-7-nitroindolines serve as a tool for the acylation of various nucleophiles. The mechanism by which the acylating species, the nitronic anhydride is formed, is not well understood. Reported here is a semiempirical AMPAC study of the reaction pathway in the ground and excited states. Results suggest an as yet experimentally unobserved ground state concerted suprafacial 1,5-sigmatropic shift pathway for the formation of the nitronic anhydride. The previously experimentally observed excited state pathway is considerably more complex. A concerted antarafacial shift is expected. However, on the S1 (lowest singlet excited state) manifold, the reaction appears to involve a shallow intermediate before proceeding by a hypothesized S1 to S0 (ground singlet) state crossing to the transition state for the concerted S0 shift, from which it likely proceeds onto a suprafacial shift to the nitronic anhydride. Triplet state behavior is explored and this system may possess a conical intersection of S0/S1/T1 potential energy surfaces. Further results explain the reactivity of the nitronic anhydride toward nucleophiles, as well as its susceptibility to protons, providing a complete mechanistic picture to explain the reaction behavior found by us and others.

KEYWORDS: nitronic anhydride, conical intersection, acylating agent

*cdirk@utep.edu

1. INTRODUCTION

Photo-cleavable aromatic nitro compounds have been used extensively as protecting groups for various functionalities in synthetic organic chemistry [1, 2]. Among them, N-acyl-7-nitroindolines stand out due to their ability to function not only as protecting groups, but also as effective acylating agents [3]. The discovery that N-acyl-5-bromo-7-nitroindolines and N-acyl-5,7-dinitroindolines undergo photosolvolysis with water, methanol, or ethanol to afford carboxylic acids or esters dates back to 1976 [4, 5]. In 1981 Patchornik and coworkers published the capability of N-peptidyl-5-bromo-7-nitroindolines to undergo aminolysis, which could be successfully used for photochemical peptide segment condensation under neutral reaction conditions [6]. Photoaminolysis was more recently used to prepare amides and carbamates [7, 8], small cyclic amides by photorelease from a solid support [9], N-glycosyl amino acids [10, 11], and for the convergent synthesis of N-glycopeptides [12]. Furthermore, peptide amides of solid support-linked 7-nitroindoline photorelease peptide thioesters in the presence of a thiol under UV-illumination [13]. Amides of 7-nitroindolines have also been used as caged compounds for the laser flash-photolytic release of amino acids [14, 15]. Morrison *et al.* suggested that N-acetyl-5-methylacetate-7-nitroindoline **1** converts to the nitronic anhydride intermediate **4** upon illumination with near UV-light (Figure 1) [16]. Intermediate **4-6** may have two distinctly different fates that are solvent-dependent leading to 7-nitroindoline **7-9** or 7-nitrosoindole **10-12**. A series of photolysis experiments with N-acetyl-5-methylacetate-7-

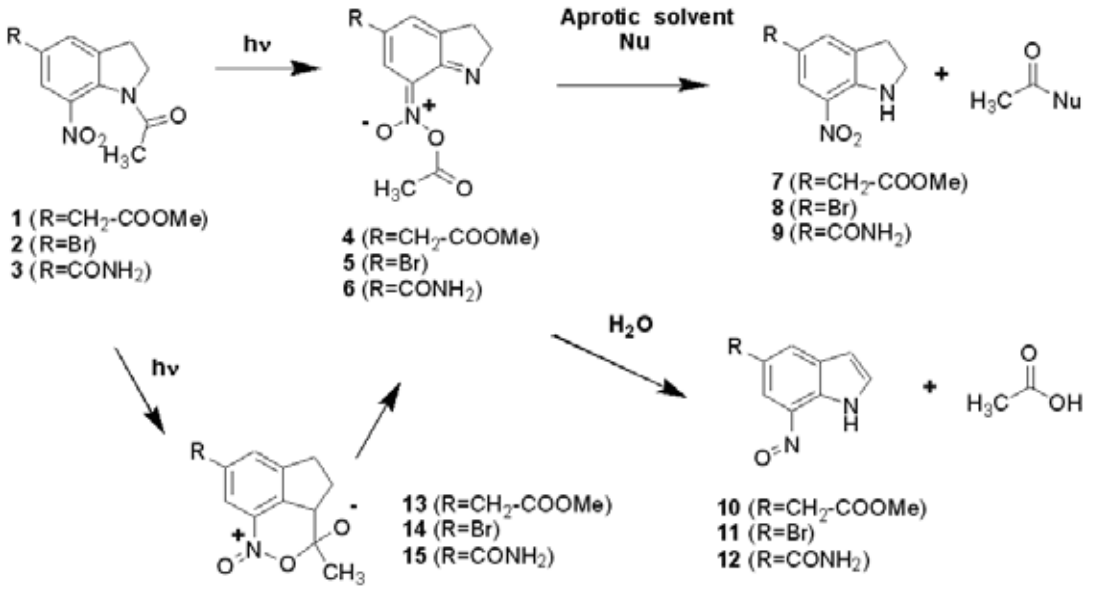

Figure 1. Photoactivation of N-acyl-7-nitroindolines and two alternative fates of intermediate (**5-8)** depending on the reaction conditions.

nitroindoline (**1**) in varying ratios of water/ acetonitrile showed that small water contents lead predominantly to nitroindoline **7,** and large water contents produce predominantly nitrosoindole **10** [16]. Both paths produce acetic acid. At low water content acetic acid is formed by hydrolysis, and at high water content by an intramolecular redox reaction.

To date, the mechanism of this important photoactivation and why certain conditions cause the formation of different products is poorly understood. We reasoned that unraveling the mechanism of the photoactivation of N-acyl-7-nitroindoline (**1-3**) may lend support for the formation of nitronic anhydride intermediate (**4-6**), which has never been isolated to date. Furthermore, study on the reactivity of **4-6** may help clarify the pathways that produce carboxylic acid and nitrosoindoles **10-12**.

Despite several studies on this photoinduced reaction, its mechanism remains mostly unknown. Several mechanistic and kinetic studies using nanosecond flash photolysis, UV-Vis spectroscopy and deuterated isotope effects attempted to unravel mechanistic details [1, 6, 14, 17]. It is generally believed that N-acyl-7-nitroindoline (**1-3**) photoreact in the presence of near UV light (350 nm) to form nitronic anhydride (**4-6)** by an acyl transfer [16, 17]. Once in this form, the nitronic anhydride can be easily attacked by a nucleophile in an aprotic solvent. However, in water, intermediate **4-6** reacts to form nitrosoindole **10-12** and a carboxylic acid. This study investigates the reaction mechanism for the formation of nitronic anhydride **5** and **6** and the conditions that lead to either the formation of nitroindoline **8** and **9**, or nitrosoindole **11** and **12** by using semiempirical computational chemistry. Studying the reactivity of intermediate **5** and **6** with nucleophiles (in this study, using water, ammonia, and a glycosylamine) may have implications on controlling the fate of species **4-6**, and thus on product formation, in the hands of an experimentalist.

The mechanism proposed by Morrison *et al.* suggested a tetrahedral intermediate (**13**) via a triplet path from the excited singlet [16]. It was not stated whether **13** existed in both the ground state and excited state, or solely in one or the other. Alternatively, one could consider a concerted antarafacial 1,5-sigmatropic shift, and this is also considered below. Key experimental features, which must be accounted for are the apparent presence of an excited state intermediate, triplet sensitization which can divert from the nitronic anhydride product, and the sensitivity to water.

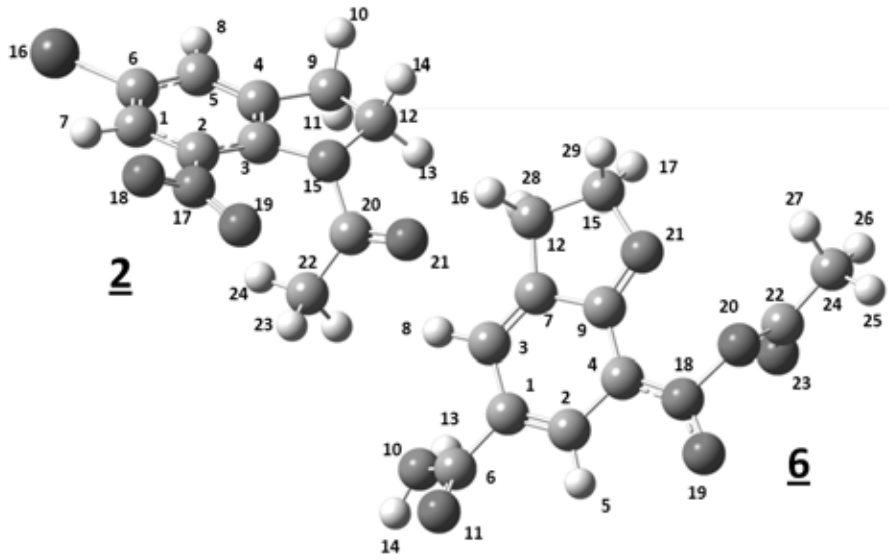

Figure 2. The PM3 RHF ground state structure **2** (**2-RG** of Figure 3) and **6** (**6-PG** of Figure 3) as arrived from SDP calculation from sigmatropic shift transition state. Note that for the numbering of **3**, the acetyl C22 is bound to N21.

2. METHODS

The AMPAC semiempirical program (Version 9.2.1 from Semichem Inc.) was used for all calculations. The parameterization for all calculations was PM3 [18-20]. Ground states were calculated using RHF (restricted Hartree-Fock) or by choosing the lowest state in a configuration interaction calculation that included all singly excited configurations. Excited states were undertaken with configuration interaction and included all singly excited configurations. Potential energy surfaces (PES) were searched/ scanned using well established methods [21-28] available in AMPAC. Points along the PES were characterized by vibrational frequency analysis. Intermediates displayed no negative vibrations, while transition states (TSs) possessed a single negative vibration. Some critical points were neither intermediates nor transition states. Reaction profiles were calculated using either the steepest descent path (SDP) [29] or the intrinsic reaction coordinate (IRC) [23] methods within AMPAC. IRC is similar to SDP, but while SDP is conducted in internal coordinates, IRC is done in Cartesian coordinates and includes a local mode calculation at each point along the PES, starting from the transition state. PES calculations were carried out on structures **2** and **3**, with the intent of finding a path to **5**, and **6**, respectively. Most results are reported for the **2** to **5** transformation, and nucleophilic substitution reactions reported for **3** and **6**. The atom numbering referred to in this work is based on the numbering established for the calculations. We provide in Figure 2 the numbering used for **2** and **6**. Selected additional calculations were performed on structures **1** and **4** as specified below. Coordinates necessary to generate structures and potential energy surfaces discussed in this investigation are reported in supplementary material.

Note for the structures shown, the presence or absence of explicit bonds does not imply presence or absence of bonding, as the graphical user interface of AMPAC may neglect to draw a bond based on a slightly long distance for the atom types.

Calculations are gas phase, except where indicated.

3. RESULTS AND DISCUSSION

3.1. Ground state results

Ground state (S0) calculation were undertaken first, and quickly lead to identifying a concerted 1,5-sigmatropic shift, apparently suprafacial (Figure 3), to the nearest oxygen atom, O19. This ground state reaction has apparently not yet been observed experimentally. For both the **2** to **5** and **3** to **6** ground state transformations, the reaction is endothermic (28.7 & 29.2 kcal/mol, respectively), with significant

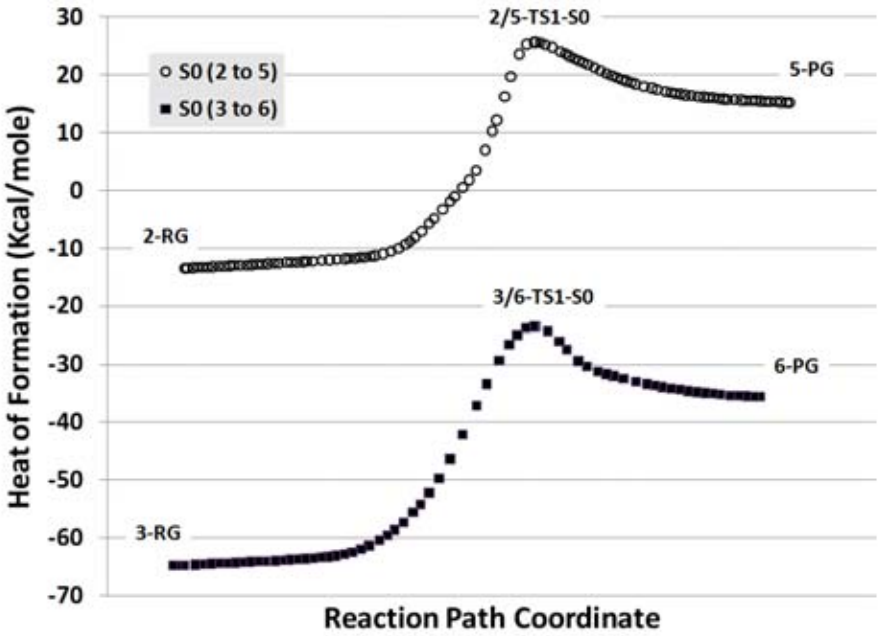

Figure 3. Steepest Descent Path or Internal Reaction Coordinate for Ground State reaction of **2** to **5** and **3** to **6**. The **2** to **5** reaction to shift of the acetyl to O19 is calculated from the transition state structure using IRC, while the **3** to **6** is calculated by SDP. The transition states have been made to coincide along the reaction coordinate. Energies are Heat of Formation enthalpies. The transition states were verified by vibrational analysis.

activation enthalpies (39.2 & 42.3 kcal/mol, respectively). Thus, neither reaction is favored in the ground state. Upon identifying the transition state, either a steepest descent path or internal reaction coordinate calculation was carried out to show that the reactant and product are connected by this transition state. Except for the energy differences that are a result of the Heat of Formation differences between **2**/**5** and **3**/**6**, the two profiles are very similar, suggesting there is little substituent effect difference of the bromo and amido substituents. Thus, further discussion will not provide duplicative analogous results for all substituents.

For both transformations, the nitro group begins slightly nonplanar (**2**: C3-C2-N17-O19 dihedral = -29.299º) to the benzene moiety, and at the transition state the angle reduces to 3.427º. The transition state (Figure 4) looks more like product than reactant as expected for a strongly endothermic reaction. For the **2** to **5** transformation, the C20-N15 distance changes from 1.470 Å in the ground state to 1.933 Å in the transition state, and is 3.117 Å in the product **5**. Observe that the ground state TS bears some structural and charge distribution similarities

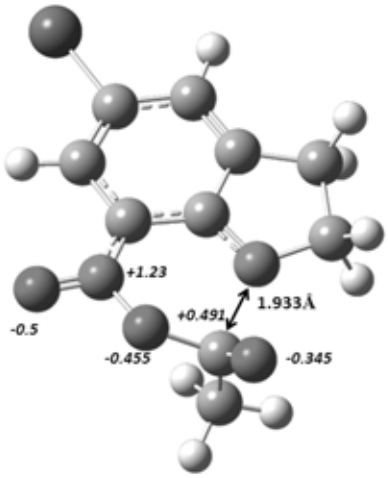

Figure 4. Transition State **2/5-TS1-S0** for the ground state shift with some Coulson charges.

to what might be expected for the intermediate (**13**) proposed by Morrison *et al.* for the excited state reaction.

One can also identify a transition state for the concerted ground shift to O18 (Figure 5). This is a

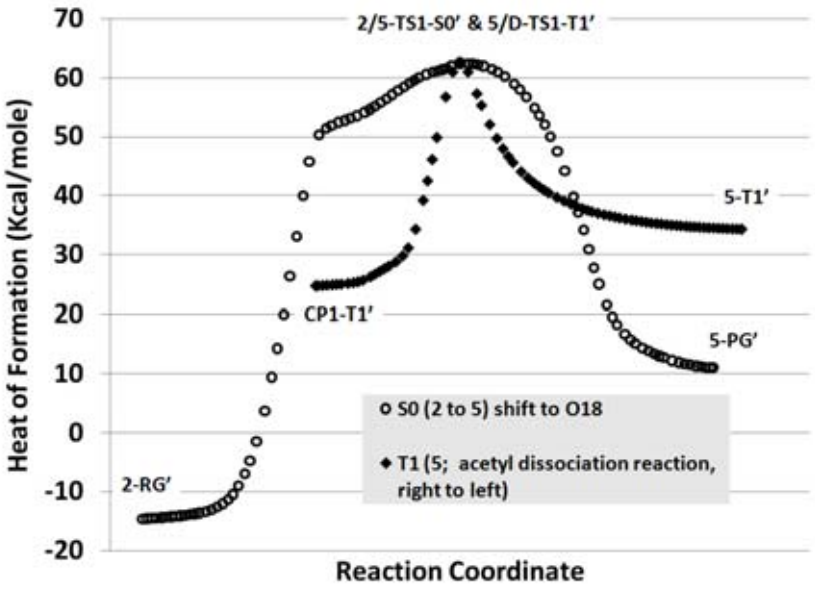

Figure 5. Concerted shift of acetyl to O18. Note the primed terms to distinguish this PES from that of Figure 3. Also included is a T1 reaction acetyl dissociation from nitronic anhydride **5-T1'**, passing through transition state **5/D-TS1-T1'** to form dissociated products **CP1-T1'**. The triplet reaction shares the same TS state structure and energy as the ground state S0 reaction.

much higher energy pathway with an activation energy of 77.0 kcal/mol. The transition state (Figure 6) is unusual and involves an excursion of the acetyl group around the nitro group. In the TS, the C20-N15 distance is 4.11 Å. The TS C20-O19 distance is 3.18 Å, while the C20-O19 distance is 2.63 Å. The starting structure (**2-RG'**) for **2** for this reaction as derived from the SDP calculation is not identical to **2-RG** derived from the SDP reaction coordinate calculation shown in Figure 3. **2-RG'** is 1.1 kcal/mol higher in energy than **2-RG**, and the nitro is significantly more twisted out of the aromatic plane; the C1-C2-N17-O18 dihedral angle is -16.7º for **2-RG**, while it is -81.3º for 3-RG'. The products, **5-PG** and **5-PG'** are also quite different with **5-PG'** being lower in energy by 4.2 kcal/mol as a rotational or cis-trans isomer of **5-PG**. Cohen *et al.* have calculated, using B3LYP/ 6-31G*, the corresponding energy difference of 1.7 kcal/mol for the nitronic anhydride derived from N-acetyl-5,7-dintroindoline [17]. The barrier to inter-conversion between **5-PG** and **5-PG'** was explored, and was found by SDP to be 20.4 kcal/mol. This is considerably lower than the barrier of 42 kcal/mol speculated by Cohen *et al.* for N-acetyl-5,7-dintroindoline, though that [17] calculation was apparently not from a relaxed PES. As can be seen in Figure 5, a T1 (lowest triplet excited state) PES crosses and intersects at the **2/5-TS1-S0'**, so that the T1 transition state (**5/D-TS1-T1'**) possesses the same structure and energy as the **2/5-TS-S0'** transition state. This will be discussed in more detail below.

Figure 6. The transition state structure (**2/5-TS1-S0'** or **5/D-TS1-T1'**) for the ground state S0 reaction coordinate shown in Figure 5.

Given the nature of the transition state for the ground reaction, the intermediate (**13**) proposed by Morrison *et al.* was checked for stability. Attempts to optimize this proposed tetrahedral intermediate failed at the ground state (S0), S1(lowest singlet excited state), and T1 implementations. S0 **13** reverts to S0 **1**, and S1 **13** reverts to S1 **1**, and T1 **13** reverts to T1 **1**, both of which are bound similarly to ground state **1**. It is possible that **13** exists in a tetrahedral form as suggested by Morrison *et al.*, somewhere on the PES, but an approximately sp^3 tetrahedral intermediate does not appear to be likely.

3.2. Singlet excited state S1 results

The excited state behavior of **1-3** are quite a bit more complex than the apparently simple ground state sigmatropic shift. Naively, in light of the ground state reaction pathway, one might anticipate an antarafacial excited state sigmatropic shift. However, such could not be found. Instead, a search of the S1 reaction surface of the **2** to **5** or **3** to **6** transformations yields reaction coordinate segments on reactant and product sides which appear to be not connected to each other in the S1 state.

Upon vertical excitation from S0, to the S1 state of **2** (**RG-S1** of Figure 7), the molecule can relax by 6.5 kcal/mol to a new structure **RS1**. When searching for pathways along the S1 PES to facilitate a **2** to **5** transformation, two major reaction components from reactant or from product, can be identified, albeit disconnected from one another. The two reaction component coordinates are also shown in Figure 7, along with the vertical and relaxed S1 points found from SDP or IRC calculation from identified transition states.

On the product (**5**) side, one can identify a reaction surface which works backwards from the excited anhydride (PS1; the acetyl is bound to O19), but halts shortly at **CP2-S1** after transition state **TS4-S1** is achieved. All points along the **CP2-S1** to **PS1** reaction profile will relax to the ground state product **5** upon de-exciting to S0, regardless of whether on the left or right hand side of the **TS4-S1** transition state. The **TS4-S1** structure is shown in Figure 8, along with the PS1 excited product (**5**) from this reaction PES fragment. Note in PS1, the anhydride is twisted out of the plane in the S1 state. From PS1 **5** to **TS4-S1** the C20-O19 bond length changes from 1.360 Å to 1.884 Å, while the N17-O19 bond length changes from 1.590 Å to 1.254 Å. At **CP2-S1** where the IRC terminates, these bond lengths become 2.258 Å (C20-O19) and 1.230 Å (N19O19), though despite the significant C-O bond breaking, even this structure will relax

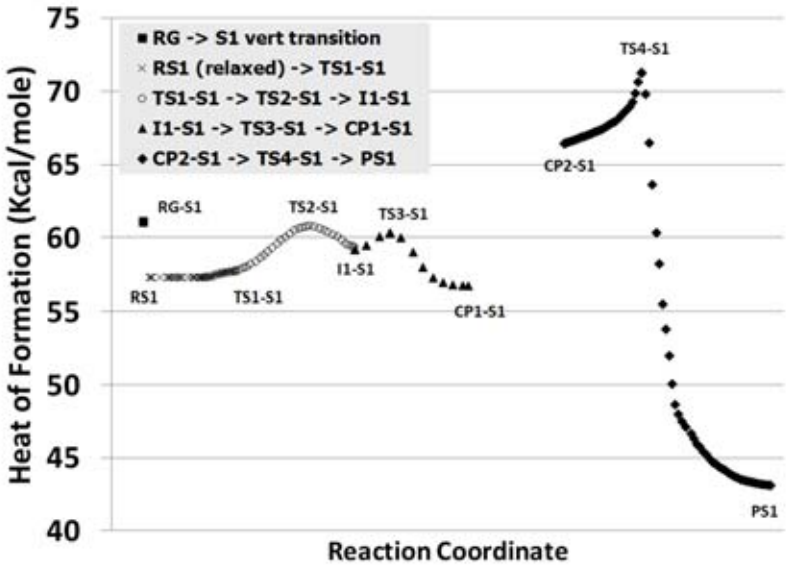

Figure 7. S1 reaction manifold for the **2** to **5** transformation. **RS1** to **I1-S1** is a continuous connected reaction coordinate, and **I1-S1** to **CP1-S1** is a continuous connected reaction coordinate, as is **CP2-S1** to **PS1**. **CP1-S1** and **CP2-S1** are not connected on the PES. **RG-S1** and **RS1** are bound as **2**, while **PS1** is bound as **5**.

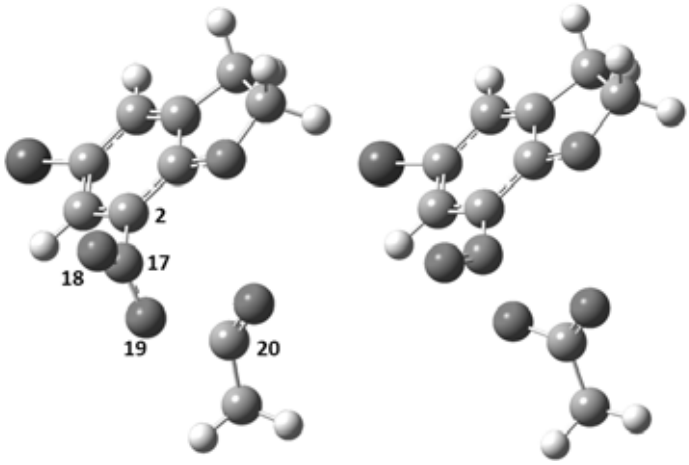

Figure 8. The structure of **TS4-S1** to left and of **PS1** to right for compound **5**. The presence or absence of drawn bonds between atoms N17-O19 or O19-C20 are an artifact of the AMPAC GUI, not a indication of the presence or absence of bonding.

to **5PG**. **CP2-S1** is a critical point on reaction coordinate that possess five negative vibrations. Hence it is not an intermediate. The IRC fails to proceed past this point.

On the reactant side of the S1 manifold, the vertical S1 structure (**RG-S1**) can further relax to **RS1**, which then can follow a reaction path to **CP1-S1**. By vibrational analysis **RS1** is an intermediate (zero negative vibrations), **RS1** passes into transition state **TS1-S1**, which involves mostly small reorganizations of the methyl and carbonyl of the acetyl group. At **TS1-S1**, another reaction path was found that leads to a higher transition state, **TS2-S1**, which then becomes an intermediate **I1-S1**. For all of these results, these reaction coordinates were found by first finding the transition states by searching the potential energy surface, then generating the reaction coordinates by IRC or SDP methods. **TS3-S1** was found to have a reaction path also to **IS1-S1**. However, the structures of **IS1-S1** derived from IRC or SDP from **TS2-S1** and **TS3-S1** are not identical, but very close in structure and energy. One presumes they are indistinguishable with room temperature induced fluctuations, and so have been assigned as a common PES point **I1-S1** linking these two reaction coordinates.

No relaxed path could be identified to link **CP1-S1** with **CP2-S1**. The S1 PES appears to have a break between these two critical points. **CP1-S1** posses four negative vibrations, while **CP2-S1** possesses five negative vibrations. Thus, they are neither intermediates nor transition states. The failure to connect **CP1-S1** to **CP2-S1** could be due to conflicting interactions with other states potential energy surfaces.

An evaluation of S1 structures with S0 wavefunctions can reveal whether there may be some crossing or touching of the S1 and S0 PESs. A crossing or touching of the surfaces, may explain why no path could be found to complete the reaction solely along the S1 manifold. Shown in Figure 9 are the energies of the S0 single point evaluations at the S1 structure, along with the S1 energies (duplication of that shown in Figure 8) for the critical region of the S1 reaction up to critical point **CP1-S1**. After progressing along the reaction coordinate from left to right, and passing through the **T3-S1** transition state, the ground state energy rises rapidly to be nearly coincident with the excited state energy. From **CP2-S1** to **PS1-S1**, the ground state energy closely matches the excited state energy except with a deviation of 1-4 kcal/mol after **TS4-S1**.

As an S1 state species, **CP1** possesses four negative vibrations, none of which seem to be associated with progress toward product. However, at S0, the **CP1** structure possesses three negative vibrations. One of these vibrations might be associated with closing the distance between the nitro O19, and

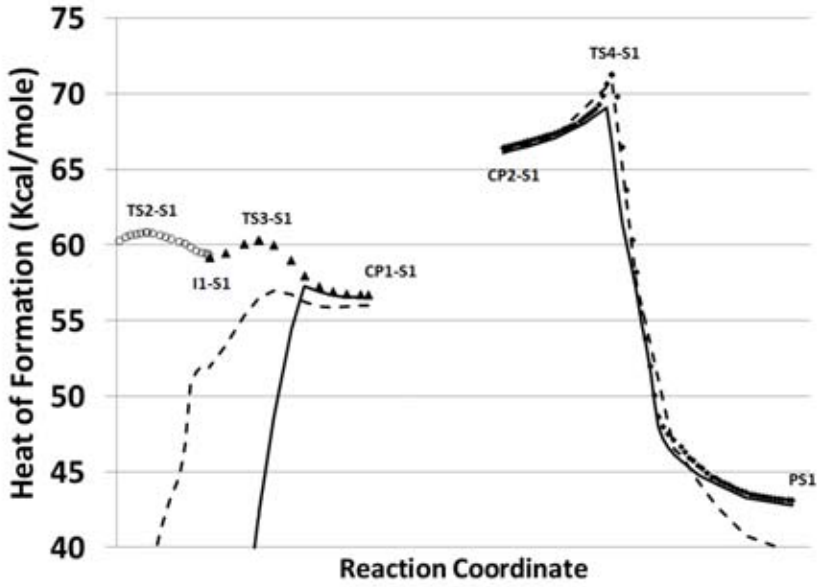

Figure 9. Calculation of the S0 and T1 energies at the S1 geometries for the **2** to **5** transformation. The S1 PES is shown zoomed slightly from Figure 6. Shown are the single point calculation of the S0 energy (solid line) and T1 energy (dashed line), calculated at the geometries of the S1 excited state.

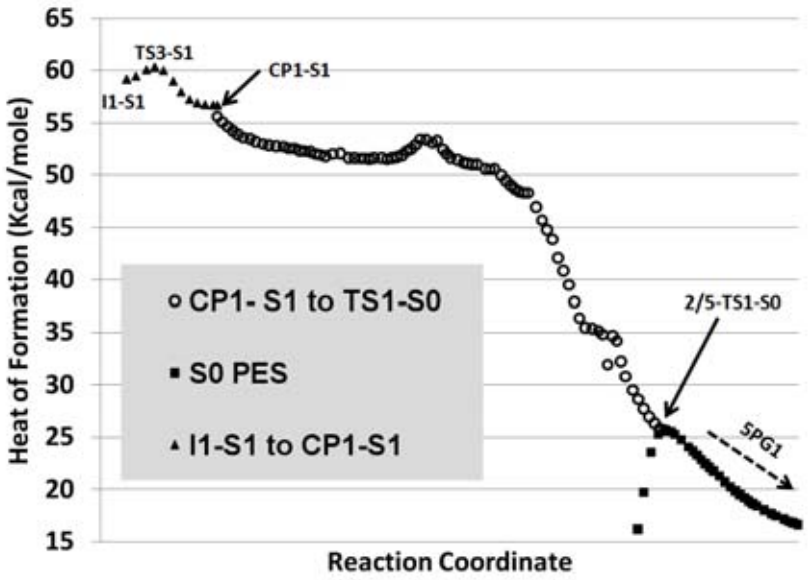

Figure 10. Results of a PES search for a path (open circles) from S1 manifold (triangles) PES point **CP1-S1** (after it crosses to the S0 manifold) to the transition state (**2/5-TS1-S0**) for the ground state sigmatropic shift reaction (squares). This path connects the data on Figure 7 with the data on Figure 3. The connection from **CP1-S1** to **TS1-S0** is not a fully relaxed or minimized PES. Thus, the path is speculative to some extent.

the carbonyl C20. If we search from **CP1** at S0 to the ground state transition state **TS1-S0**, using the method of Liotard [21] executed by the FULLCHN keyword of AMPAC 9.2 (Chapter 7 AMPAC 9.2 user guide), we can find a path (Figure 10) that may connect the two. However, this path is not a relaxed SDP or IRC coordinate, and is not a firm proof that the two can be connected. Still it provides

some support for the possibility that an S1 to S0 path exists to reach the product without the need to pass through the energetically costly **TS4-S1** transition state. Overall, the results imply that S1 crosses to S0 to complete a net suprafacial reaction. The **CP2-S1** to **PS1** PES segment is likely uninvolved in completing the photochemical reaction to convert **2** to **5.**

3.2.1. The I1-S1 intermediate

Morrison *et al.*'s work on the transformation of **1** to **4** suggested the presence of a short lived intermediate, which they suggested had the form of **13**. The results from the present investigation do suggest a true intermediate **I1-S1** with no negative vibrations, the structure of which is shown in Figure 11. Note that the structure for **I1-S1** for the **2** to **5** transformation is different (otherwise neglecting the difference in substituent at the 5-position) from that proposed earlier [16] for the **1** to **4** transformation. The acetyl is weakly bound to either the indoline N or nitro oxygens, and it appears both nitro O atoms play some role in bonding the acetyl.

The corresponding **I1-S1** intermediate for the **1** to **4** transformation was found, verified to have no negative vibrations, and served as the basis for configuration interaction calculation of the electronic absorption properties. Morrison *et al.* [16] determined that in 99% CH_3CN 1% H_2O, the transient absorbed at 415 nm, while in 100% H_2O, it was determined to absorb at 450 nm. The **I1-S1** structure for **1** was obtained from PM3, all singly excited configurations optimization in the S1 state in the AMSOL [30, 31] model reaction fields of pure water and acetonitrile. All structures refined to intermediates with zero negative vibrations. The results of the calculations are reported in Table 1.

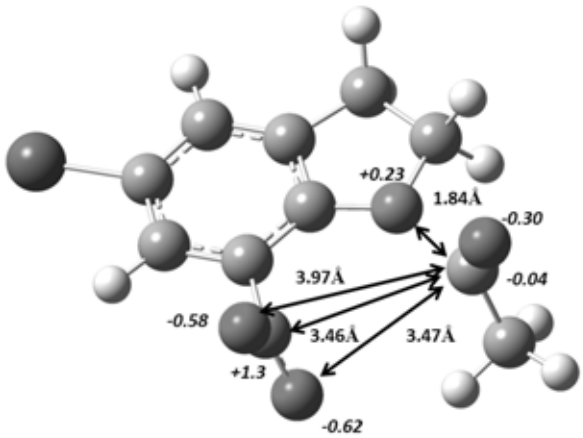

Figure 11. The I1-S1 intermediate from Figure 7. Coulson charges are in italics.

Note in Table 1 the significantly different structural parameters for the SM5.2 acetonitrile optimization relative to the others. Remarkably, this structure is still found to be bound with no negative vibrations. However, the lowest vibration is at just 5-6 cm^{-1}, so this is a very weakly bound species. It seems unlikely this could represent a real intermediate structure, and so data for this simulation will be neglected in the continuing discussion.

The SM5C acetonitrile simulation predicts a relatively dominant transition in the visible at 415 nm, coincident with experimental observation. However, while the SM5.2 water simulation has a dominant transition at 457 nm, also remarkably close to the experimental value, the SM5C water simulation places the dominant transition in the visible at 408 nm. The results are consistent with experiment, but matching electronic absorption transitions is hardly very convincing evidence on its own, so these results might be considered fortuitous and insufficiently conclusive.

3.3. Triplet pathways

3.3.1. Relaxed PES triplet reactions

The triplet T1 pathway (Figure 12) for **2** is similar to the singlet S1 path for **2** in that the reactant and product sides could not be connected along a continuous PES. The reactant side shows a steep transition state to an endothermic outcome at **I1-T1**, which results in the acyl being dissociated as a weakly bound intermediate (lowest positive vibration of 14 cm^{-1}). Low Coulson charges on the N15 (-0.039) and the C20 (+0.093), which are separated by 3.73Å in CP1-T1 (C20-O18: 6.53 Å ; C20-O19: 5.66 Å), suggest a weakly bound biradical formation. A similar result is obtained in the case of compound **3**, though the separation is smaller, 3.35 Å. If access to **RT1** is most likely through intersystem crossing from S1, it seems likely that **I1-T1** will not competitively be produced relative to **CP1-S1** given the higher activation energy barrier to **I1-T1** along the triplet manifold than to access **CP1-S1** along the S1 manifold.

Table 1. Calculated structural and UV absorption data of the **I1-S1** intermediate for **1** in state **S1**. Structures were optimized in state **S1** either under the SM5C or SM5.2 models of the AMSOL solvent model, using PM3, and all singly excited configurations. Atom numbers referred to are as labeled in Figure **1** for **2**, neglecting the difference in substituents. f_{osc} is the calculated oscillator strength for the peak at λ_{max} wavelength (nm). Only nonzero transitions at four significant digits with wavelength greater than 320 nm are presented. Negative transitions are to the ground state.

	CH_3CN; SM5.2	CH_3CN; SM5C	H_2O; SM5.2	H_2O; SM5C
C20-N15(Å)	5.04	1.89	1.92	1.90
C20-N17(Å)	6.04	3.39	3.52	3.39
C20-O18(Å)	5.36	3.94	4.09	3.95
C20-O19(Å)	6.82	3.25	3.42	3.25
λ_{max} (f_{osc})	564(0.0005) 473(0.0822) 366(0.0001) 366(0.3238) 333(0.0039) 332(0.0005) 321(0.0008)	-1029(0.0006) 967(0.0018) 635(0.0005) 582(0.0017) 546(0.0007) 415(0.0106) 394(0.0005) 393(0.0003) 363(0.0019) 362(0.0122) 335(0.0001) 320(0.0610) 320(0.0581)	-860(0.0007) 969(0.0038) 750(0.0002) 667(0.0016) 662(0.0008) 513(0.0002) 459(0.0020) 457(0.0105) 450(0.0001) 393(0.0015) 386(0.0179) 354(0.0002) 362(0.0006) 343(0.0001) 334(0.0022) 326(0.1647) 324(0.0003)	-1076(0.0006) 959(0.0021) 623(0.0005) 571(0.0017) 533(0.0008) 473(0.0001) 408(0.0106) 387(0.0003) 387(0.0004) 358(0.0019) 356(0.0121) 331(0.0001) 322(0.0693)

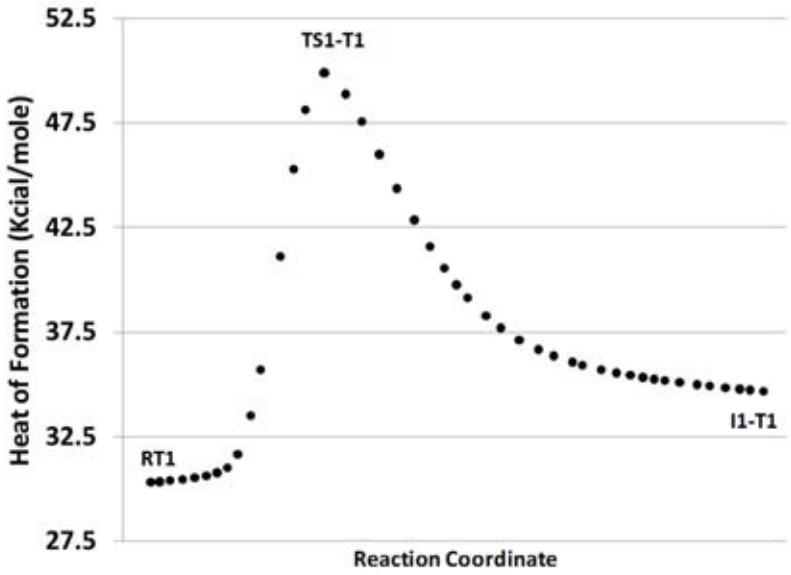

Figure 12. The relaxed PES for the reaction of **2** in the T1 state to form a weakly bound intermediate **I1-T1**.

On the product side of the reaction, excitation to the T1 state provides a T1 acetyl dissociation pathway from the nitronic anhydride (**5-T1'**; Figure 5). Dissociation is even more strongly supported here than for **I1-T1**, as **CP1-T1'** possesses two negative vibrations. Curiously, this path shares an identical transition state with the ground state concerted shift to O18 discussed earlier. The two reaction coordinates are shown in Figure 5 with the transitions states being coincident in structure, energy and reaction coordinate.

In either case, starting from reactant or product, we do not identify a triplet acetyl shift reaction to produce the nitronic anhydride **5** from the N-acetylindoline **2**. From either side of the reaction, reactant or product, the triplet state seems to lead to a species that could readily lead to acetyl dissociation.

3.3.2. Singlet/Triplet state crossing

If we calculate the T1 energy at the S1 geometries, we again see a similar effect that we saw with S0 calculations at S1 geometries. As the S1 reaction approaches **CP1-S1**, the triplet energy climbs to be almost coincident with S1 (Figure 9). This suggests that within the same region of the PES where S1/S0 crossing may occur, one could also see S1/T1 crossing. However, it could be presumed that the intersystem crossing rate from S1 to T1 will be slower than the internal conversion rate from S1 to S0, making T1 production relatively less competitive with S0 production. Triplet sensitization reactions [16] have shown that **1** can be converted to **7** and **10** by way of a presumed triplet pathway. This is entirely consistent with and supported by the results presented here which suggest that the acetyl group could possibly dissociate when **2** or **3** follow a triplet path, and that the nitronic anhydride product (**5-T1'**; Figure 5) is also subject to dissociation in the triplet state.

It is also straightforward to implicate an apparent triplet intermediate as done by Morrison *et al.* [16]. for the production of the anhydride by considering that if the T1, S1, and S0 share the same region of the PES (near or after **CP1-S1** in Figure 7), it would be possible experimentally to detect the T1 species that might then go on to the nitronic anhydride by crossing to S0 and then following the path (Figure 10) to the **2/5-TS1-S0** transition state. Thus, while the triplet is not necessary to form the nitronic anhydride, it can occasionally become a temporary excursion on the way to the nitronic anhydride by a dynamic T1/S1/S0 equilibrium. The fraction of T1 that exists relative to S1 or S0 may depend on the spin orbital coupling between the three species, and might be influenced by substituents and solvents.

3.4. Nucleophilic attack on the nitronic anhydride and N-Acyl-7-nitroindoline

The reactivity of nitronic anhydride 6 and N-acyl-7-nitroindoline 3 towards nucleophiles was studied by simulating nucleophilic substitutions on the carbonyl group of the acyl group on both molecules. The simulations were carried on the S0 state assuming gas phase conditions. The selected nucleophiles were water, ammonia and ß-d-N-acetylglucosaminylamine. The reaction was divided into two steps; the first step being the nucleophilic attack and formation of the acetylated nucleophile with the release of the nitroindoline moiety, the second step being the deprotonation of the acetylated nucleophile moiety by the nitroindoline moiety. Figure 13 shows a scheme of the reactions that were examined.

Table 2 shows the results of the nucleophilic attack calculations, including step 1 and step 2 as outlined in Figure 13. The results bear out that the nucleophilic attack on the nitronic anhydride **6** is much more favored than the attack on the N-acyl-7-nitroindoline **3**. The activation energy for the attack is also much lower in the nitronic anhydride confirming the kinetic benefits of undergoing the photochemical acyl transfer prior to the nucleophilic attack. The energy drop after the proton transfer and formation of the 7-nitroindoline **9** is substantial in both electrophiles. The reactions with both ammonia and the glycosylamine as a nucleophile yielded two step reactions as shown in Figure 13. However, the reactions involving water as a nucleophile generated one step reactions for both electrophiles. The reaction coordinate for the nitronic anhydride reaction with water is shown in Figure 14. The simulations indicate that the water molecule attacks the carbonyl group and donates a proton in one step. The water molecule has just the right size to enter the pocket formed between

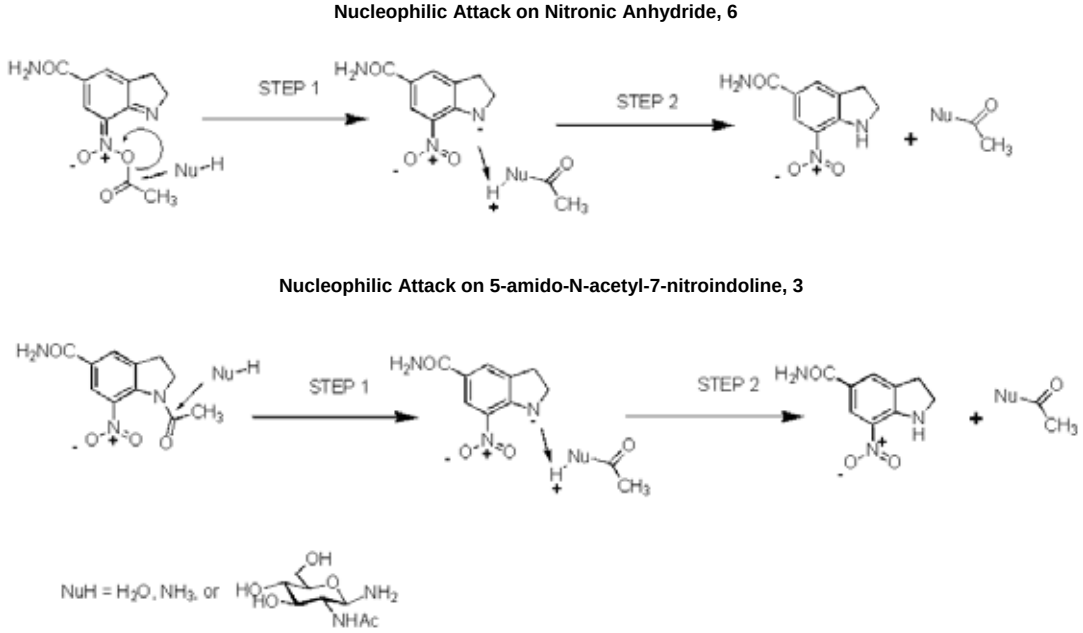

Figure 13. Reactions simulated for either nucleophilic attack upon the acetyl C of nitronic anhydride **6** or upon acetylnitroindoline **3**. Both the nucleophilic attack (STEP 1) and subsequent deprotonation reactions (STEP 2) were studied. Nucleophiles were water, ammonia and the amine N of β-N-acetylglucosaminylamine.

Table 2. Showing the results of the calculations for the reactions in Figure 13. The reaction using nitronic anhydride **6** as an electrophile is clearly more thermodynamically favored than that of N-acyl-7-nitroindoline **3**. Water is a special case where both the attack and deprotonation steps occurred as a concerted reaction. All data is in Kcal/mole.

	Electrophile							
	Nitronic anhydride 6				**N-acyl-7-nitroindoline 3**			
	Nucleophilic Attack		Deprotonation Step	Overall Reaction	Nucleophilic Attack		Deprotonation Step	Overall Reaction
Nucleophile	**E_{act}**	**$\Delta\Delta H_f$**	**$\Delta\Delta H_f$**	**$\Delta\Delta H_f$**	**E_{act}**	**$\Delta\Delta H_f$**	**$\Delta\Delta H_f$**	**$\Delta\Delta H_f$**
Ammonia	14.40	-2.10	-21.59	-40.16	38.97	9.52	-25.61	-16.09
β-D-N-acetylglucosaminylamine	27.78	-1.37	-41.71	-43.07	36.91	22.87	-32.76	-9.89
Water	18.65	-	-	-40.15	60.17	-	-	-10.72

the acyl group in both electrophiles and the nearest nitrogen atom. Figure 15 shows the transition state structures for both reactions. This remarkable ability of a water molecule to enter this pocket and act in such a concerted fashion, along with the higher activation for bulky nuclelophiles such as a glycosylamine (making them relatively noncompetitive) seems to suggest a reason to account for the sensitivity of N-acyl-7-nitroindolines to competitively form carboxylic acids even when water is present in less than 1% concentration and under aprotic solvents [16].

3.5. Protonation of nitronic anhydride and formation of 7-nitrosoindoline cations

Figure 1, shows that when the nitronic anhydride reacts in water it is thought to decompose into a 7-nitrosoindole molecule and the free carboxylic acid. Water can act as a source of protons by equilibrium, or protonic acid is produced when

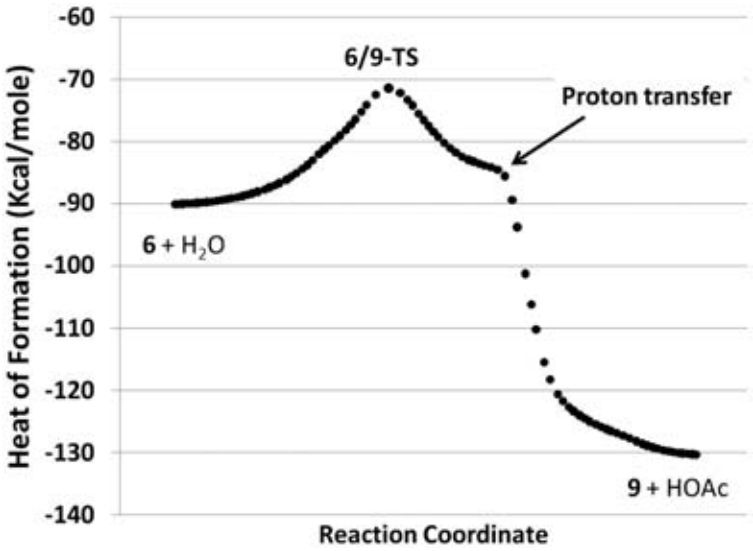

Figure 14. The reaction coordinate for the nucleophilic attack of water on nitronic anhydride **6**. There is a single transition state (structure pictured in Figure 15), and proton transfer occurs within the fully concerted reaction coordinate.

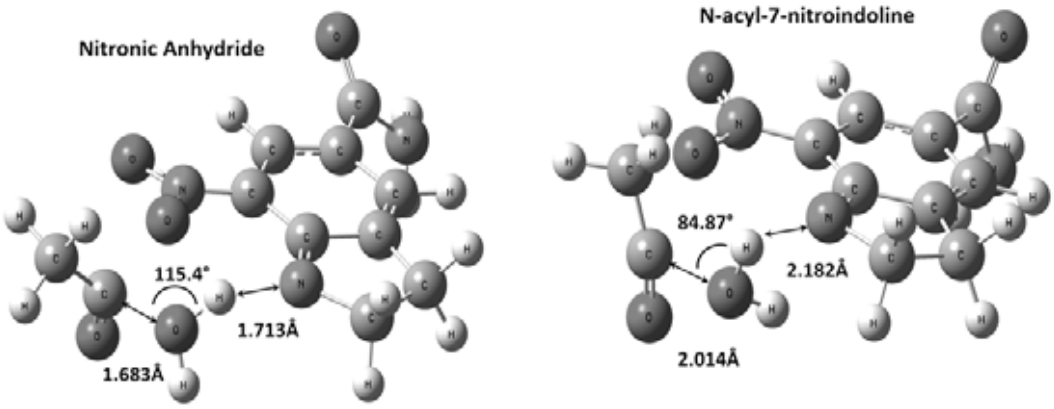

Figure 15. Image showing the transition states of the reaction of water with the two electrophiles **3** (right) and **6** (left). Notice the alignment of the strong presence of the hydrogen bond between nitrogen atom in the indoline molecule and the hydrogen atom in water. Further along the PES the hydrogen atom is fully bonded to the nitroindoline and the carboxylic acid is formed. The water molecule is just about the right size to be able to coordinate with the electrophile in this fashion to enable nucleophilic displacement and proton transfer to occur in a single step.

water undertakes a nucleophilic attack creating the carboxylic acid as described in the above section. To simulate the effects of acid on nitronic anhydride, the molecule **6** was protonated on all three possible oxygen atoms associated with the nitronic anhydride moiety, then allowed to relax to assume the lowest energy structure. The structures were optimized in the ground state with PM3 semiempirical model using all singly excited configurations over all orbitals along with the AMSOL [30, 31] SM5C solvation model using dimethylsulfoxide as a solvent. The results are shown in Figure 16. Protonation of the oxygens that are part of the ester bond (O20 and O23) automatically leads to dissociation and formation of cationic nitroso species (**24**, Figure 17) and the

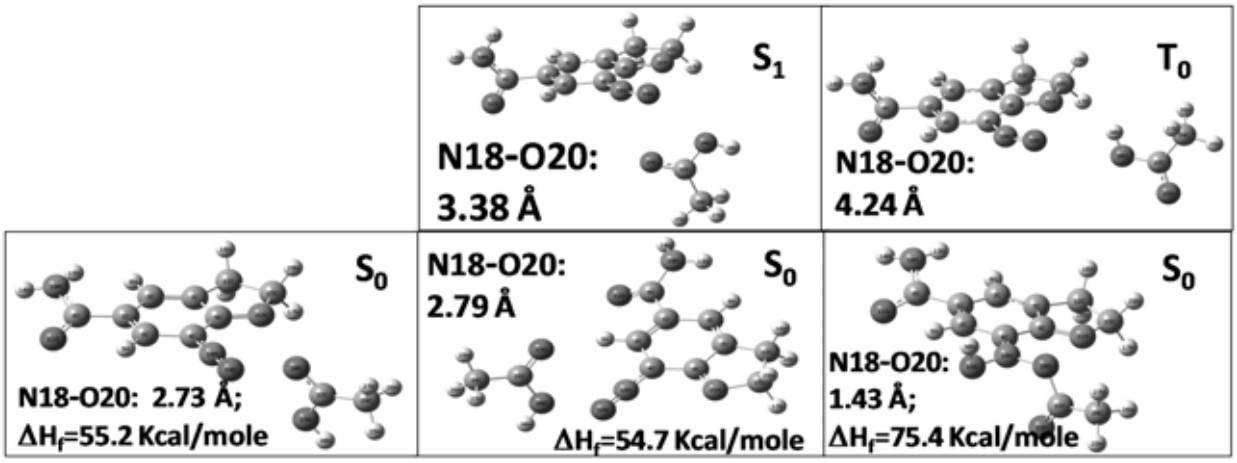

Figure 16. The effects of nitronic anhydride protonation in the ground and excited states. The designated O atom was protonated, then the structure was energy minimized with SM5C DMSO solvent simulation. The bottom row shows the outcome of protonation of each of the oxygen atoms of **6** potentially involved in dissociation. From left to right are the ground state protonations of O23, O20, and O19 in the ground state. Note that protonation of O19 is relatively very unfavored and will not lead to dissociation. In the top row, protonations are of O20 in the S1 and T1 states. If acetic acid dissociated, the distance to the closest HOAc O atom, protonated or not, is given.

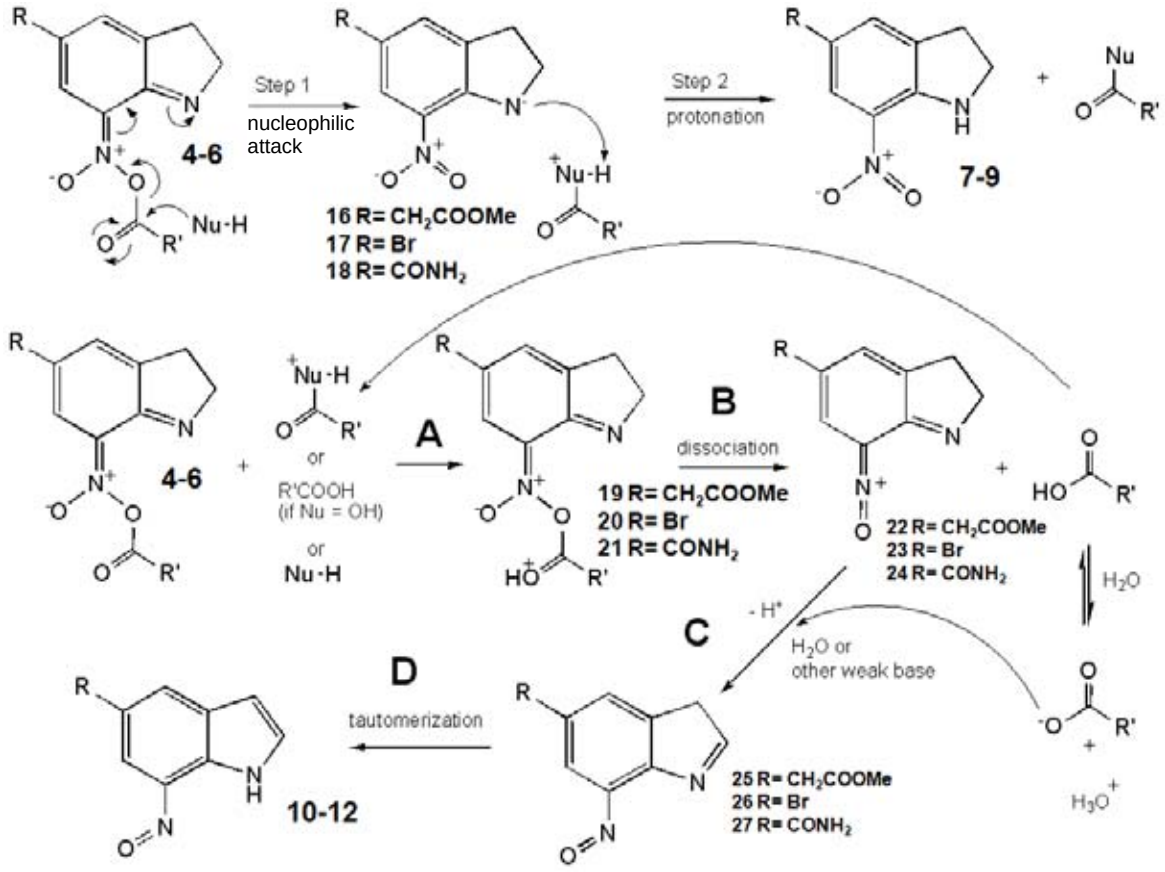

Figure 17. Complete reaction scheme which shows the production of nitroindoline and nitrosoindole.

free carboxylic acid. Meanwhile, protonation on O19 does not lead to dissociation but to a structure which is 20 kcal/mol higher in energy than the other two (after relaxing to dissociated species), implying protonation of O20 and O23 is more likely. The protonation of nitronic anhydride on oxygen 20 in the two other likely possible electronic states S1 and T1 was also investigated, and in all cases, the nitronic anhydride is unstable to dissociation into carboxylic acid and nitroso species **24**. The results for all of the protonation reactions are shown in Figure 16. In concert with our findings regarding the concerted action of water, trace proton may also make the nitronic anhydride very short lived, and enables a ready path (Figure 17) to the nitroso derivative **12**.

3.6. Final conversion of nitroso species 22-24 to nitrosoindole (10-12)

It has been shown in previous sections that protonation of nitronic anhydride leads to the dissociation of the molecule into positively charged nitroso species **22-24** and free carboxylic acid. However, as stated in Figure 1 the nitrosoindole and the free carboxylic acid are the end products when the reaction is carried out in water. Under this condition, the nucleophilic attack on the nitronic anhydride yields excess of protons that in the best of cases is absorbed by the nitroindoline and thus completing the nucleophilic substitution (as in step 2 in Figure 17) or the extra proton can be donated to another nitronic anhydride (to form **19-21**; step **A** in Figure 17) inducing the decomposition (step **B** in Figure 17) of nitronic anhydride to form **22-24** and more carboxylic acid. This acid can dissociate and protonate more nitronic anhydride, and dissociation will increase as the concentration of acid increases. As more acid dissociates, the conjugate base of the acid can deprotonate (step **C** of Figure 17) the positively charged **22-24** to form **25-27** that can easily tautomerize (**D**, Figure 17) under an aqueous environment to form **10-12**.

4. CONCLUSIONS

The reactions that can create nitronic anhydrides from the acylnitroindolines are complex. A thermal ground state reaction appears to simply be a thermodynamically and kinetically unfavorable sigmatropic shift, though this has not yet been observed experimentally. The S1 excited state pathway is multifaceted. An intermediate, **I1-S1**, has been identified, consistent with earlier experimental results, though it is not calculated here to be precisely tetrahedral in character [16] as initially speculated as **13-15** in Figure 1. As the reaction proceeds after the **I1-S1** intermediate, there appears to be a small energy barrier to reach a region of the PES (**CP1-S1**) which may permit crossing or touching of the S0 state with the S1 state. It is most likely the conversion to the nitronic anhydride proceeds from this point by crossing to the ground state reaction surface. Note that the vertical transition energy is probably more than sufficient to reach this part of the PES, so the reaction is facile, as observed. However, given the weak bonding of the intermediate **I1-S1**, one might wonder whether a group larger than methyl for the acyl as calculated here might cause the intermediate to be much more poorly bound. Thus acyl groups bound to long or bulky peptide chains might be considerably different in their reactivity to form the anhydride. The methods used here could clarify the relative proclivity to form the nitronic anhydride as well as the relative reactivity of the anhydrides of specific acyl substituents.

We also present results which support S1 and T1 state crossing or touching, which could facilitate the formation of a T1 species. Note that the T1 should be prone to dissociation, leading to a diversion from the nitronic anhydride pathway, which is also consistent with experimental observations. The PES results are certainly rich in their intricacy. For instance, besides the likely state crossing to lead to the product, the nitronic anhydride product itself displays a possible T1/S0 sharing of a transition state. From the reactant side, the T1/S1/S0 intersection permits a triplet state to form that can then still go on to the nitronic anhydride product by intersystem crossing back to either S1 or S0.

The nitronic anhydride is a very reactive species, and it is prone to nucleophilic attack. The attack of water is especially favored due to the water being of the appropriate size to undergo a concerted reaction to form the carboxylic acid and

donate the extra proton to the nitroindoline. This explains the unusual sensitivity to traces of moisture, and a pathway to nitroindoline **7-9** from the nitronic anhydride in the presence of moisture. By computation, protonation of the nitronic anhydride in any state seems to result in the formation of carboxylic acid and nitrosoindole **10-12**. Thus, while water alone provides a path to the nitroindoline, acid from any source can provide a ready path to the nitrosoindole, which is available by straightforward textbook chemistry from the cationic nitroso species **22-24**. The destruction of the nitronic anhydride and production of nitrosoindole not only by water, but by any protic solvents can thus be readily explained. Isolation and identification of the nitronic anhydride should take into consideration the apparent extraordinary susceptibility of the compound to moisture and acid.

Obviously, while these results are quite intriguing, they beg a high accuracy ab initio study, as well as further experimental exploration. Semiempirical methods, while helpful for a survey like this investigation, are probably insufficient to address some issues with adequate accuracy. It seems likely an excited state crossing exists, and would be verified at higher accuracy. However, the fine details may be more circumspect. In particular, the validity and nature of the intermediate **I1-S1** needs to be better characterized, as well as the details on the path of the suggested S1/S0 state crossing to the ground state transition state, and the role and fate of the triplet species. If the **I1-S1** intermediate is real, then one naturally wonders, as considered above, what effects larger acyl groups might experience given weak bonding. In addition, this system is highly interesting because of the possible S1/T1/S0 conical intersection. If such a three state intersection occurs, the reaction dynamics may possess some richer subtleties that haven't been discovered as yet.

ACKNOWLEDGEMENTS

We thank Dr. Andrew Holder and Semichem Inc, for technical support with AMPAC, and Dr. Katja Michael's research group for support and comments. We would also like to thank Dr. Jorge Gardea-Torresedey and the Department of Chemistry for generous support of the site license for AMPAC. This research was supported in part by the Getty Conservation Institute (C.W.D) and by NSF grant CHE-0719538 (K.M.).

REFERENCES

1. Pillai, V. N. R. 1980, Synthesis, 1-26.
2. Pillai, V. N. R. Organic Photochemistry, 1987, Padwa, A. (Ed.) Marcel-Dekker: New York, 225-323.
3. Debieux, J.-L. and Bochet, C. G. 2010, J. Phys. Org. Chem., 23(4), 272-282.
4. Amit, B., Ben-Efraim, D. A. and A. Patchorik, A. 1976, Journal of the American Chemical Society, 98, 843-844.
5. Goissis, G., Erickson, B. W. and Merrifield, R. B. 1977, Proceedings of the 5th American Peptide Symposium, 559-561.
6. Pass, S., Amit, B. and Patchornik, A. 1981, Journal of the American Chemical Society, 103, 7674-7675.
7. Helgen, C. and Bochet, C. G. 2001, Synlett, 1968-1970.
8. Helgen, C. and Bochet, C. G. 2003, Journal of Organic Chemistry, 68, 2483-2486.
9. Nicolaou, K. C., Safina, B. S. and Winssinger, N. 2001, Synlett, 900-903.
10. Simo, O., Lee, V. P., Davis, A. S., Kreutz, C., Gross, P. H., Jones, P. R. and Michael, K. 2005, Carbohydrate Research, 340, 557-566.
11. Vizvardi, K., Kreutz, C., Davis, A. S., Lee, V. P., Philmus, B. J., Simo, O. and Michael, K. 2003, Chemistry Letters, 32, 348-349.
12. Kaneshiro, C. M. and Michael, K., 2006, Angewandte Chemie International Edition, 45, 1077-1081.
13. Hogenauer, T. J., Wang, Q., Sanki, A. K., Gammon, A. J., Chu, C. H., Kaneshiro, C. M., Kajihara, Y. and Michael, K. 2007, Org. Biomol. Chem., 5, 759-762.
14. Papageorgiou, G., Lukeman, M., Wan, P. and Corrie, J. E. T. 2004, Photochem. Photobiol. Sci., 3, 366-373.
15. Papageorgiou, G., Ogden, D. C., Barth, A. and Corrie, J. E. T., 1999 Journal of the American Chemical Society, 121, 6503-6504.
16. Morrison, J., Wan, P., Corrie, J. E. T. and Papageorgiou, G. 2002, Photochem. Photobiol. Sci., 1(12), 960-969.

17. Cohen, A. D., Helgen, C., Bochet, C. G. and Toscano, J. P. 2005, Organic Letters, 7, 2845-2848.
18. Stewart, J. J. P. 1989, J. Comput. Chem., 10(2), 221-64.
19. Stewart, J. J. P. 1989, J. Comput. Chem., 10(2), 209-20.
20. Stewart, J. J. P. 1991, J. Comput. Chem., 12(3), 320-41.
21. Liotard, D. A. 1992, International Journal of Quantum Chemistry, 44, 723-741.
22. Liotard, D. A. P. and Penot J. P. 1981, Numerical Methods in the Study of Critical Phenomena, Berlin: Springer-Verlag.
23. Fukui, K., 1970, J. Phys. Chem., 74(23), 4161-3.
24. Tachibana, A. and Fukui, K. 1978, Theor. Chim. Acta, 49(4), 321-47.
25. Ishida, K., Morokuma, K. and Komornicki, A. 1977, J. Chem. Phys., 66(5), 2153-6.
26. Ralston, A. and Wilf, H. S. 1960, Mathematical Methods for Digital Computer, J. Wiley & Sons, New York.
27. McIver, J. W. Jr. and Komornicki, A. 1971, Chem. Phys. Lett., 10(3), 303-6.
28. McIver, J. W. Jr. and Komornicki, A. 1972, J. Amer. Chem. Soc., 94(8), 2625-33.
29. Miller, W. H., Handy, N. C. and Adams, J. E. 1980, J. Chem. Phys., 72(1), 99-112.
30. Dolney, D. M., Hawkins, G. D., Winget, P., Liotard, D. A., Cramer, C. J. and Truhlar, D. G. 2000, J. Comput. Chem., 21(5), 340-366.
31. Hawkins, G. D., Cramer, C. J. and Truhlar, D. G. 1998, J. Phys. Chem. B, 102(17), 3257-3271.